## Title
FURTHER STUDY ON A MAGNETICALLY-FILTERED MULTICUSP ION SOURCE



## Authors
Ehlers, K.W.
Leung, K.N.

## Publication Date
1982-02-01

LBL-14066
Preprint

Lawrence Berkeley Laboratory
UNIVERSITY OF CALIFORNIA



Accelerator & Fusion
Research Division

Submitted to Review of Scientific Instruments

# FURTHER STUDY ON A MAGNETICALLY-FILTERED MULTICUSP ION SOURCE

K.W. Ehlers and K.N. Leung

February 1982



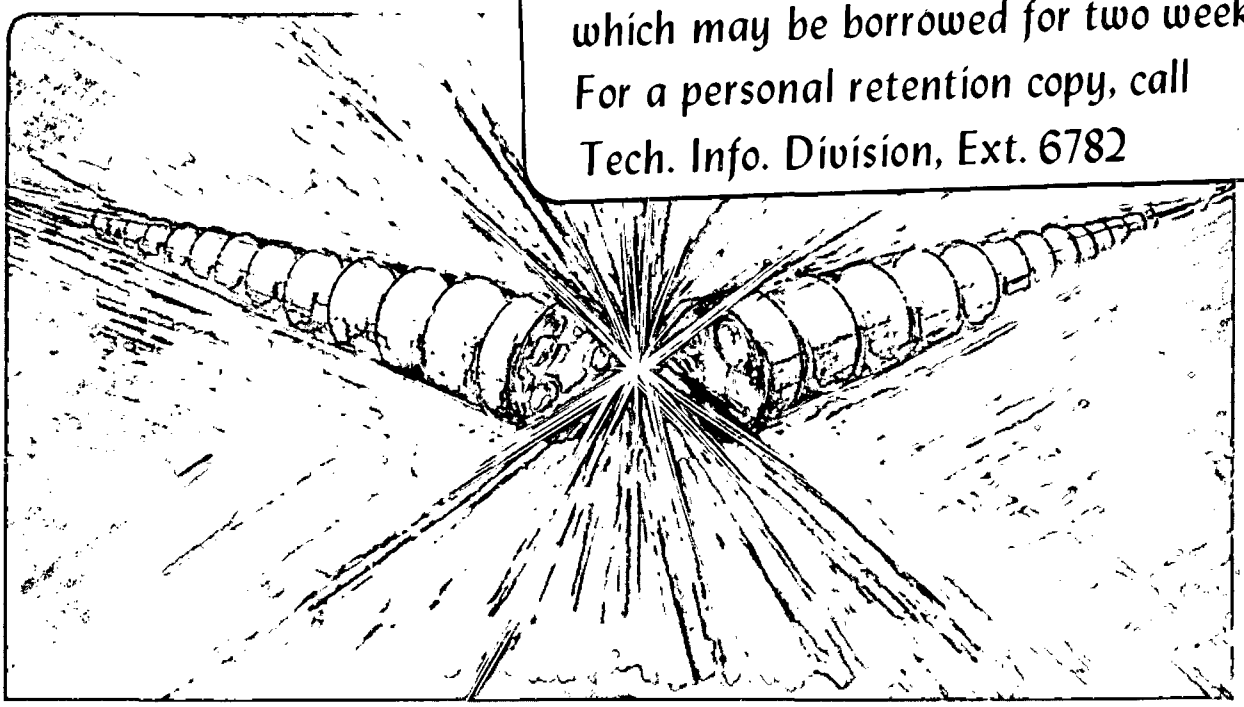

Prepared for the U.S. Department of Energy under Contract DE-AC03-76SF00098

## DISCLAIMER

# Further Study on a Magnetically-Filtered Multicusp Ion Source[+]

K. W. Ehlers and K. N. Leung

Lawrence Berkeley Laboratory
University of California
Berkeley, CA 94720

## Abstract

An optimized permanent magnet filter geometry has been determined for a multicusp ion source operated with hydrogen gas. By applying a negative bias potential to the plasma grid, energetic secondary electrons are produced which can generate molecular hydrogen ions in the extraction chamber and thus reduce the $H^+$ ion fraction in the extracted beam. Both the atomic species percentage and the ion current density can be improved by the addition of 16 eV electrons into the extraction chamber. It is also observed that once started, the discharge can be maintained with only the extraction chamber and the plasma grid acting as the anode. Thus the total discharge current can pass through the filter in the form of cold electrons.

+ This work is supported by the Director, Office of Fusion Energy, Development & Technology Division, of the the U.S. Department of Energy under Contract No. DE-AC03-76SF00098.

## Introduction

Recently, it was found that the addition of a permanent magnet filter arrangement to a multicusp ion source geometry could improve the atomic hydrogen ion fraction, the source operability and the plasma density profile at the extraction plane.[1] The filter provides a limited region of transverse magnetic field which is made strong enough to prevent the energetic electrons in the source chamber from crossing over into the extraction chamber but it is weak enough that some plasma does diffuse into the extraction region. Since only very cold electrons are found in the extraction chamber, ionization processes are unlikely to take place. It has been observed that the $H^+$ ion percentage increases with the field strength of the filter. But the plasma density in the extraction chamber is always less than that in the source chamber, and this reduction is a function of the magnitude and thickness of the filter B-field, as well as to the filter's geometric transparency. Thus the cost of obtaining a very high atomic ion component is the sizable reduction in the total extractable ion current.

In this paper, an attempt has been made to optimize the filter geometry so that a reasonably large ion current density to the extractor is obtained along with the high percentage of atomic hydrogen ions. The effect of a large negative bias voltage applied to the plasma grid on the electrical efficiency of the source and to the hydrogen ion species distribution was also investigated. In addition, the injection of 16 eV electrons into the extraction chamber has resulted in a further enhancement of the $H^+$ ion concentration as well as an increase in the

extractable ion current density. We have also observed that, once started, the source can be operated by using only the plasma grid and the extraction chamber as the anode for the discharge. This demonstrates that the cold electrons observed in the extraction chamber pass through the filter with relative ease.

## I. Experimental Apparatus

Figure 1 shows a schematic diagram of the ion source which consists of two cylindrical stainless-steel chambers (20 cm diam) separated by a thin insulator ring and a permanent magnet filter.[1] In order to increase the geometric transparency and to provide adequate cooling, the filter was constructed by inserting square ceramic magnet rods into copper tubes through which a square broach had been passed. Since the magnets rested on the four broached grooves, their orientations could not change and water was then run through the remaining space to provide adequate cooling.

Ten columns of samarium-cobalt magnets ($B_{max} \approx 3.6$ kG) were mounted on the external surface of both chambers, forming continuous line-cusps parallel to the source axis for primary electron and plasma confinement.[2] The source chamber (24 cm long) together with the filter becomes essentially a completely enclosed multicusp geometry with one leaky side, and as it contains the energetic primary electrons it is therefore the ion source chamber where all ionization occurs. The extraction chamber (6 cm long) which has one end enclosed by a three-grid extractor, contains a plasma with only low-energy electrons. In normal

operation, the filter and the two chambers were connected together electrically. A steady state hydrogen plasma was produced by primary electrons emitted from six 0.05 cm-diam tungsten filaments located in the source chamber. These filaments were biased at -80 V with respect to the chamber wall and the filter which served as the anode for the discharge. Plasma parameters in the two chambers were obtained by Langmuir probes.

In order to study the hydrogen ion species distribution, a small beam was extracted (~300 eV) from the extraction chamber by means of a standard Berkeley accel-decel three electrode system. The extracted beam was then analyzed by a compact magnetic-deflection mass spectrometer[3] located just outside the extractor. In this experiment, the pressure in the vicinity of the mass spectrometer was sufficiently low ($\sim 1 \times 10^{-4}$ Torr) that dissociation and charge-exchange processes were minimized in the region between the extractor and the spectrometer. The actual pressure inside the source was approximately $1.5 \times 10^{-3}$ Torr.

## II. Optimization of Filter Geometry

The plasma density in the extraction chamber is always less than that in the source chamber. This reduction is a function of the magnitude and thickness of the filter B-field, as well as the filter's geometric transparency. The effective transparency, the floating potential of the plasma grid and the hydrogen ion species distribution have been investigated for four different filter geometries and the results are summarized in Table I.

The effective transparency is defined as the ratio of the ion saturation current density measured by a probe in front of the extraction grids with and without the filter for the same discharge conditions. Although Filter (4) gives the highest transparency, the floating potential $V_f$ of the plasma grid is lower than those of the other filters. This low $V_f$ indicates the presence of high energy electrons near the extractor. These high energy electrons, which have succeeded in penetrating through the filter, are capable of producing ions in the extraction chamber, thus increasing the molecular component. Other effects of a low $V_f$ will be discussed in the next section.

The highest $H^+$ ion percentage can be obtained by employing Filter (2). However, because of the stronger B-field, this filter has an effective transparency of only 43%. Filter (3), in turn, provides a reasonable balance between transparency, high $H^+$ ion percentage, and plasma grid floating potential. This filter, shown in Fig. 2, was therefore chosen as the optimized configuration. All measurements made for the following sections of this paper were obtained with this "optimized" filter geometry. A plot of the B-field as a function of the axial distance through the center of this filter is shown in Fig. 3. The data presented in Table I were all obtained with the source operated at 80 V and 10 A. As more discharge power is applied, the effective transparency remains the same, but the atomic ion fraction continues to increase. Figure 4 shows this change in species distribution for this particular filter as a function of discharge current $I_d$. It can be seen that the atomic component $H^+$ has increased to about 72% with $I_d$ = 80 A, at which point, the ion current density at the extractor was approximately 0.08 A/cm$^2$.

## III. Plasma Grid Potential

In general, a multicusp ion source can be operated with the plasma grid of the extractor connected to the anode, electrically floating, connected to the negative cathode terminal or biased even more negative than the cathode potential by means of an extra power supply. The electrical efficiency of the source is low if the plasma grid is biased at anode potential. Higher electrical efficiency can be achieved if the potential of the plasma grid is made sufficiently negative to reflect the primary ionizing electrons back to the volume plasma to ionize the background gas. We have investigated the effect of biasing the plasma grid negatively with respect to the chamber wall in the presence of a filter. Figure 5 shows a plot of the plasma grid current $I_g$ as a function of the grid bias voltage $V_b$. The current $I_g$ increases monotonically with $V_b$ and does not saturate even when $V_b$ is greater than the discharge voltage $V_d = 80$ V.

As the grid bias is increased, positive ions strike the grid with increasing energy, and the increase in $I_g$ is partly due to the resulting increase in the secondary electron emission current. These secondary electrons have an energy of a few electron-volts when they leave the grid surface, but they gain more energy as they accelerate across the sheath into the extraction chamber plasma. If the final energies of these secondary emission electrons exceed the ionization potential energy of the neutral gas, then additional ions will be formed in the extraction chamber, resulting in a higher grid current $I_g$.

If $I_1$ is the ion current flowing from the source chamber into the extraction chamber, $\alpha$ is the fraction of that current which impacts the

plasma grid, $\gamma$ is the coefficient of secondary electron emission of the plasma grid, and $I_2$ is the ion current lost to the anode and the plasma grid from the additional plasma generated in the extraction chamber by the secondary emission electrons, then for a first order approximation, the current collected by the grid can be expressed as:

$$I_g = \alpha I_1 + \gamma\alpha I_1 + \alpha I_2 \tag{1}$$

The production rate of ions in the extraction chamber depends on the energies of the secondary emission electrons which in turn vary with the potential of the plasma grid. If multiple ionization are taken into consideration, then[4]

$$I_2 = \gamma\alpha I_1(R_1 + R_1R_2 + R_1R_2R_3 + - - -) \tag{2}$$

where $$R_n = \left[r_e L/2Vn_o\,\sigma_{in} + (1 + \sigma_{en}/\sigma_{in})\right]^{-1}$$

Here, $r_e$ is the electron Larmor radius and L is the total length of the line cusps, V is the volume of plasma in the extraction chamber, $n_o$ is the neutral density, and $\sigma_{in}$ and $\sigma_{en}$ are the ionization and excitation cross-section for the energetic electron after it has performed (n - 1) ionization processes. Thus the normalized grid current $I_g/\alpha I_1$ can be calculated by using the known cross-sections for ionization and excitation for $H_2$ [5] and the measured value of $\gamma$[6]. (We have assumed that $\gamma(H^+) = \gamma(H_2^+) = \gamma(H_3^+)$ for the same ion energy[7]). Figure 6 shows a plot of $I_g/\alpha I_1$ versus the grid bias voltage $V_b$. It can be seen that the calculated grid current also increases monotonically with $V_b$. The calculated grid current increases by approximately 14% as $V_b$ is changed from 80 to 120 V,

while the measured value (Fig. 5) increases by about 19%. The calculated change should be less than the measured result in that it has not taken into account the production of secondary electrons by other processes - such as photoelectric effects.

Figure 7 shows probe characteristics obtained in both the source and extraction chambers with the plasma grid floating and again with the grid biased at -80 V relative to the anode. The probe traces in Fig. 7(a) shows that the density, potential and electron temperature of the source-chamber plasma are essentially the same for either of the two modes of operation. However, the probe characteristics in Fig. 7(b) shows that the density of the plasma in the extraction chamber is increased by about 21% when the grid potential is changed from floating to -80 V. There is no significant change in the plasma potential in this chamber, but the big decrease in floating potential when the grid is biased at -80 V clearly indicates that a substantial number of high energy electrons have been introduced into the extraction chamber. Since the energetic electrons do not come from the source chamber through the filter, the increase in high energy electron population must due to the generation of energetic secondary electrons from the plasma grid. These energetic electrons in turn, are responsible for the increase in plasma production in the extraction chamber.

By applying a large negative bias voltage to the plasma grid, one can increase the plasma density in the extraction chamber and therefore increase the extractable ion current. However, the secondary emission electrons can be expected to generate more $H_2^+$ ions in the extraction region. This effect is illustrated by the spectrometer output signal

shown in Fig. 8. For the same discharge voltage and current, the percentage of $H_2^+$ increases from 25% to 34% when the grid is changed from a floating potential of about -10 V to a bias voltage of -100 V relative to the chamber. At the same time, the $H^+$ ion percentage drops from 32% to 27%.

Thus, if a high percentage of atomic species is desired, the plasma grid should not be biased or left floating at a potential more negative than the ionization potential of molecular hydrogen (~16 eV). In addition, a very negative grid bias or floating potential will increase the power loading and the sputtering rate of the plasma grid by ions falling through the sheath. This in turn will increase the impurity content of the source plasma.[8] As the negative bias increases, the tendency for the grid to arc to the positive plasma increases, and bias voltages as high as -100 V are exceedingly difficult to maintain unless the plasma density is quite low.

## IV. Low Energy Electron Injection

In a previous paper, we demonstrated that the $H^+$ ion percentage could be further enhanced by injecting additional electrons (from a second set of filaments) with energies approximately equal to 16 eV into the source chamber of the magnetic filter geometry.[1] These electrons are too cold to produce $H_2^+$ ions, but they can dissociate hydrogen gas molecules as well as the molecular ion species $H_2^+$ and $H_3^+$. This technique produces no significant change in the ion current density at the extraction plane and therefore can be of interest only after one has obtained the desired extraction ion current density and wishes to

increase the atomic component without altering the ion current density.

We have now investigated the effect of putting these sub-ionizing electrons into the extraction chamber. Figure 9 shows Langmuir probe traces obtained in the two chambers before and after 5 A of 16 eV electrons were injected into the extraction chamber from six 0.05-cm-diam tungsten filaments. The background plasma is maintained by 80 V, 10 A discharge in the source chamber. Figure 9(a) shows that there is no significant change in plasma density in the source chamber except that the plasma potential drops by about 0.8 V. On the other hand, the plasma potential in the extraction region decreases by about 2 V as shown in Fig. 9(b). As more low-energy electrons are added, one would expect to see $V_p$ become more negative. The plasma density remains about the same but the electron temperature $T_e$ has increased from 2.3 to 3.8 eV by the addition of these 16 eV electrons. Because of this increase in $T_e$ [9], and also due to the change in species distribution, the ion current density to the extraction grid is estimated to increase by approximately 30%.

The spectrometer output signals in Fig. 10 show that the $H^+$ ion species increases from 33% to 40% by injecting the sub-ionizing electrons into the extraction region. Since these electrons cannot produce $H_2^+$ ions, the increase in $H^+$ concentration probably comes from the increase in the rate of dissociating molecular ions $H_2^+$ and $H_3^+$ that have passed through the filter into the extraction chamber.

## V. Plasma Grid and Extraction Chamber as the Anode

In normal operation, the plasma grid is electrically floating and

the anode for gas discharge is provided by the two chamber walls and the magnetic filter. With the switch S (shown in Fig. 1) open, it is not possible to start the plasma by just using the plasma grid and the extraction chamber as the anode. But once the discharge is started with the switch S close, the plasma can still be maintained when the switch S is opened. Since the source chamber and the filter are both electrically floating, the plasma grid and the extraction chamber now become the only anode for the discharge. No significant change has been observed on the discharge voltage (80 V) and the discharge current (5 A) before and after the switch S is opened.

The B-field of the filter is strong enough to keep the primary electrons from getting into the extraction chamber. Therefore, it is mainly the cold background plasma electrons that carry the total discharge current to complete the circuit. The exact process of how the low-energy electrons are able to penetrate through the B-field of the filter is not yet fully understood. However, their presence in the extraction region is found to be closely related to the amount of positive ions that come through the filter.[10] The potential of the source chamber plasma is approximately 1.5 V more positive than that of the extraction chamber plasma before and after the switch S is opened. This potential gradient is in the favorable direction for accelerating positive ions into the extraction chamber. By gradually reducing the discharge voltage, it is found that the difference in plasma potential between the two chambers also decreases.[10] The plasma finally extinguishes itself when the two plasma potentials are approximately equal, which occurs when the discharge voltage is about 60 V.

## Acknowledgments

We would like to thank H. Tolleth for all the technical assistance and members of the LBL neutral beam group for valuable discussions. The skillful technical work of L. A. Biagi, H. H. Hughes and members of their groups is also gratefully acknowledged. This work is supported by the Director, Office of Fusion Energy, Development & Technology Division, of the U.S. Department of Energy under Contract No. DE-AC03-76SF00098.

## References


1. K. W. Ehlers and K. N. Leung, Rev. Sci. Instrum. 52, 1452 (1981).
2. K. N. Leung, T. K. Samec, and A. Lamm, Phys. Lett. A 51, 490 (1975).
3. K. W. Ehlers, K. N. Leung, and M. D. Williams, Rev. Sci. Instrum. 50, 1031 (1979)
4. K. N. Leung, R. D. Collier, L. B. Marshall, T. N. Gallaher, W. H. Ingham, R. E. Kribel, and G. R. Taylor, Rev. Sci. Instrum. 49, 321 (1978).
5. S. C. Brown, Basic Data of Plasma Physics (MIT Press, Cambridge, MA, (1966).
6. J. A. Ray and C. F. Barnett, J. Appl. Phys., 50, 6516 (1979).
7. D. Hasselkamp, K. G. Lang, A. Scharmann, and N. Stiller, Nucl. Instrum. and Meth. 180, 349 (1981).
8. Y. Okumura and Y. Ohara, Proceedings of the Third Neutral Beam Workshop, Gatlinburg, TN (Oct., 1981).
9. K. N. Leung, R. D. Collier, G. R. Taylor, and R. E. Kribel, Appl. Phys. Lett. 31, 154 (1977).
10. K. W. Ehlers and K. N. Leung, Appl. Phys. Lett. 38, 287 (1981).

## Figure Captions

Fig. 1 Schematic diagram of the multicusp ion source with the permanent magnet filter.

Fig. 2 The optimized magnetic filter. Permanent magnets are installed inside the water-cooled tubings.

Fig. 3 A plot of the magnetic field across the plane of the filter (shown in Fig. 2) in between two magnet rods.

Fig. 4 Hydrogen ion species distribution as a function of discharge current for the optimized filter. Discharge voltage is maintained at 80 V.

Fig. 5 The measured grid current as a function of grid bias voltage with $V_d$ = 80 V and $I_d$ = 10 A.

Fig. 6 The calculated grid current as a function of grid bias voltage.

Fig. 7 Langmuir probe characteristics obtained in the source and extraction chambers with the plasma grid (A) floating and, (B) biased at -80 V relative to the anode.

Fig. 8 The spectrometer output signal showing the hydrogen ion species with the plasma grid (A) floating, (B) biased at -80 V and, (C) biased at -100 V relative to the anode.

Fig. 9 Langmuir probe characteristics obtained in the source and extraction chambers for the case (A) without and, (B) with 5 A of 16 eV electrons injected into the extraction chamber.

Fig. 10 The spectrometer output signal showing the hydrogen ion species for the case (A) without and, (B) with 5 A of 16 eV electrons added to the extraction chamber.

Table I. Source characteristics for four different filter geometries. Data were obtained with $V_d$ = 80 V and $I_d$ = 10 A.

| Filter | Magnet cross-section ($mm^2$) | Magnet spacing (cm) | Maximum B-field (gauss) | $\int B\,dr$ (gauss-cm) | Effective transparency (%) | Plasma grid floating potential (V) | $H^+ : H_2^+ : H_3^+$ |
|---|---|---|---|---|---|---|---|
| no filter | - | - | - | - | 100 | -56 | 24 : 35 : 41 |
| 1 | 3.5 x 3.5 | 4 | 40 | 89 | 68 | -15 | 30 : 17 : 53 |
| 2 | 4.5 x 4.5 | 4 | 76 | 166 | 43 | -2 | 41 : 15 : 44 |
| 3 | 4.5 x 4.5 | 6 | 35 | 104 | 70 | -10 | 35 : 19 : 46 |
| 4 | 4.5 x 4.5 | 8 | 20 | 89 | 80 | -25 | 26 : 25 : 49 |

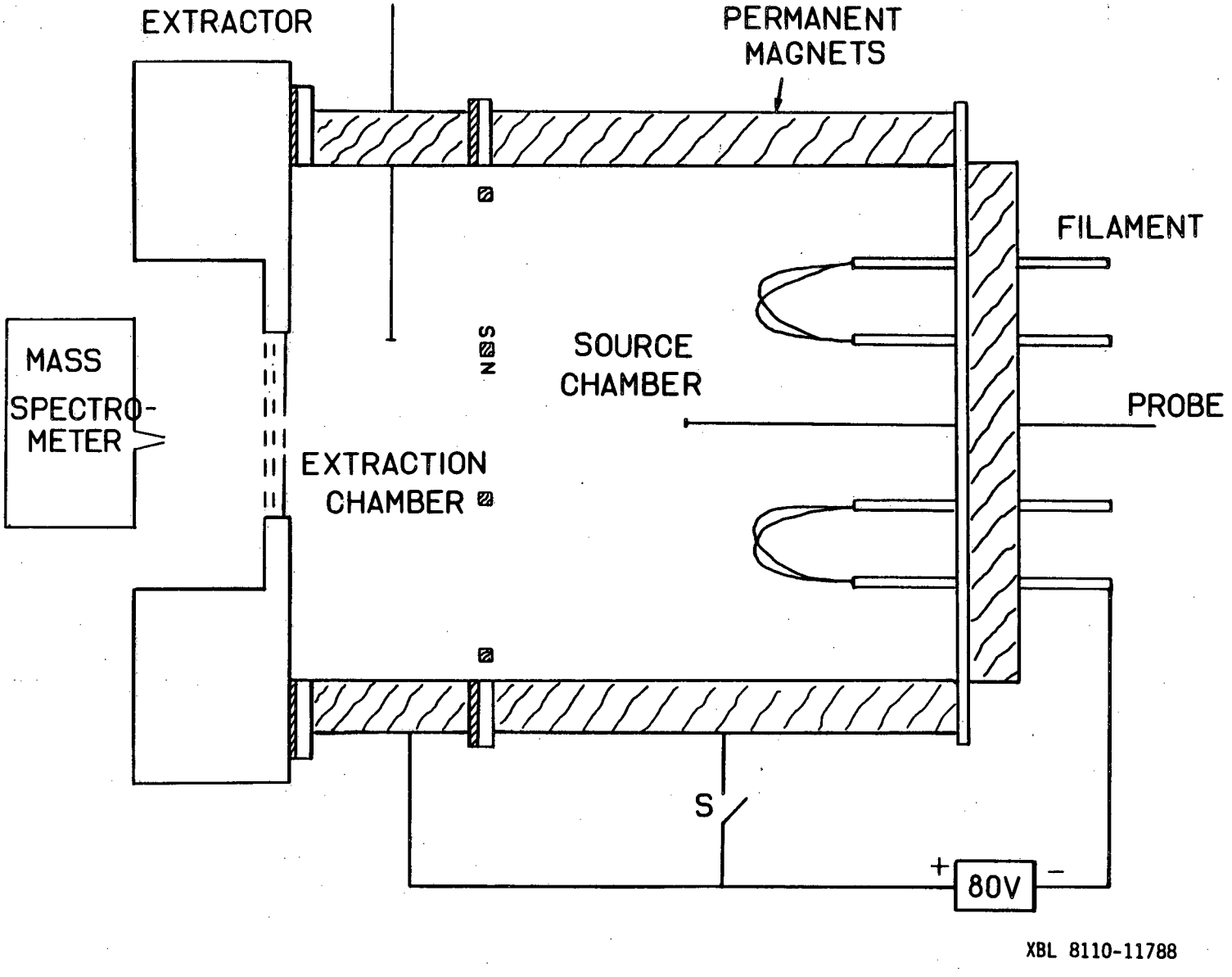
EXTRACTOR
PERMANENT MAGNETS
FILAMENT
MASS SPECTRO-METER
N
S
SOURCE CHAMBER
PROBE
EXTRACTION CHAMBER
S
+
80V
−
XBL 8110-11788

Fig. 1

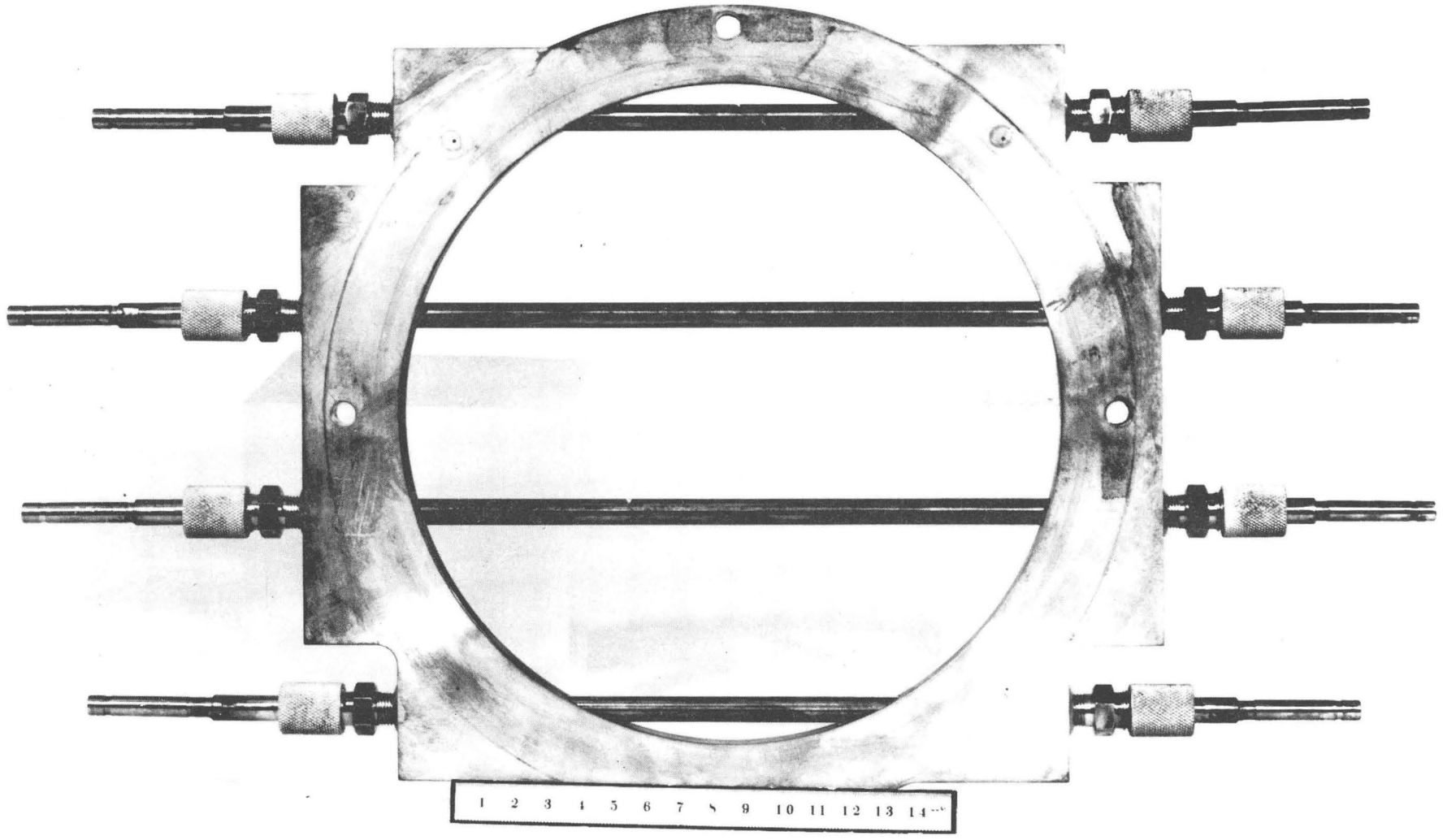


Fig. 2

CBB 814-3321

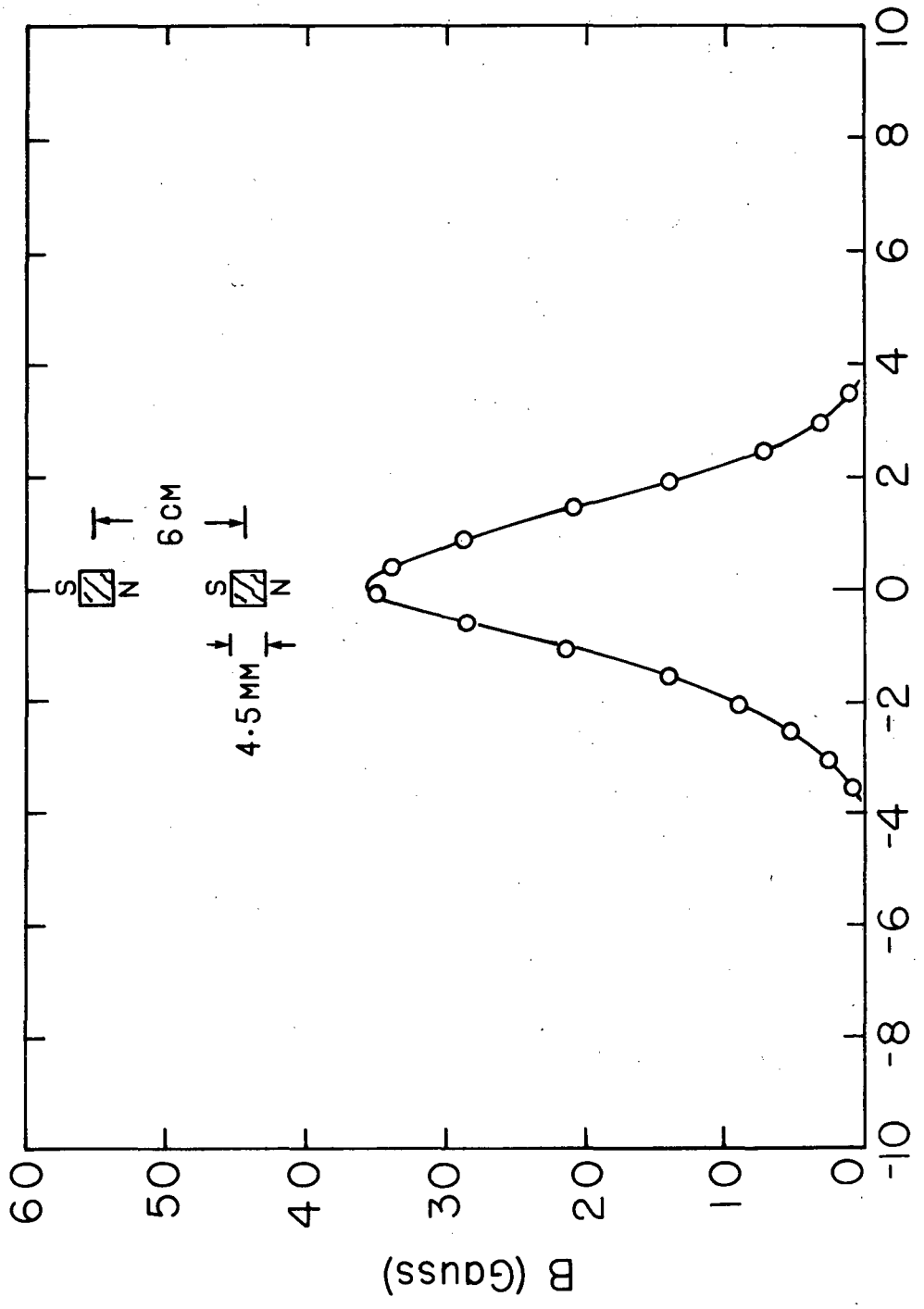


XBL 814-9139

Fig. 3

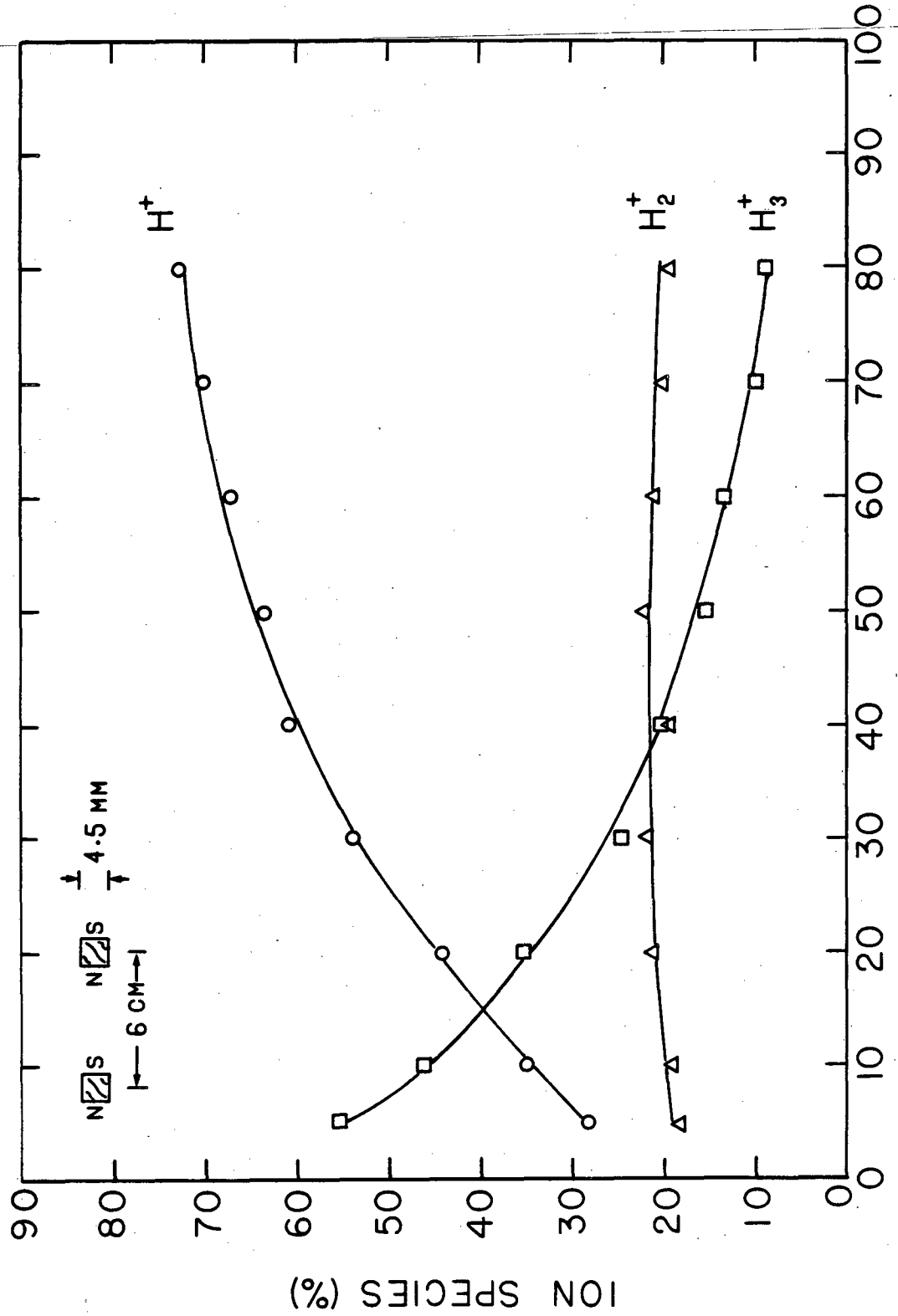


Fig. 4

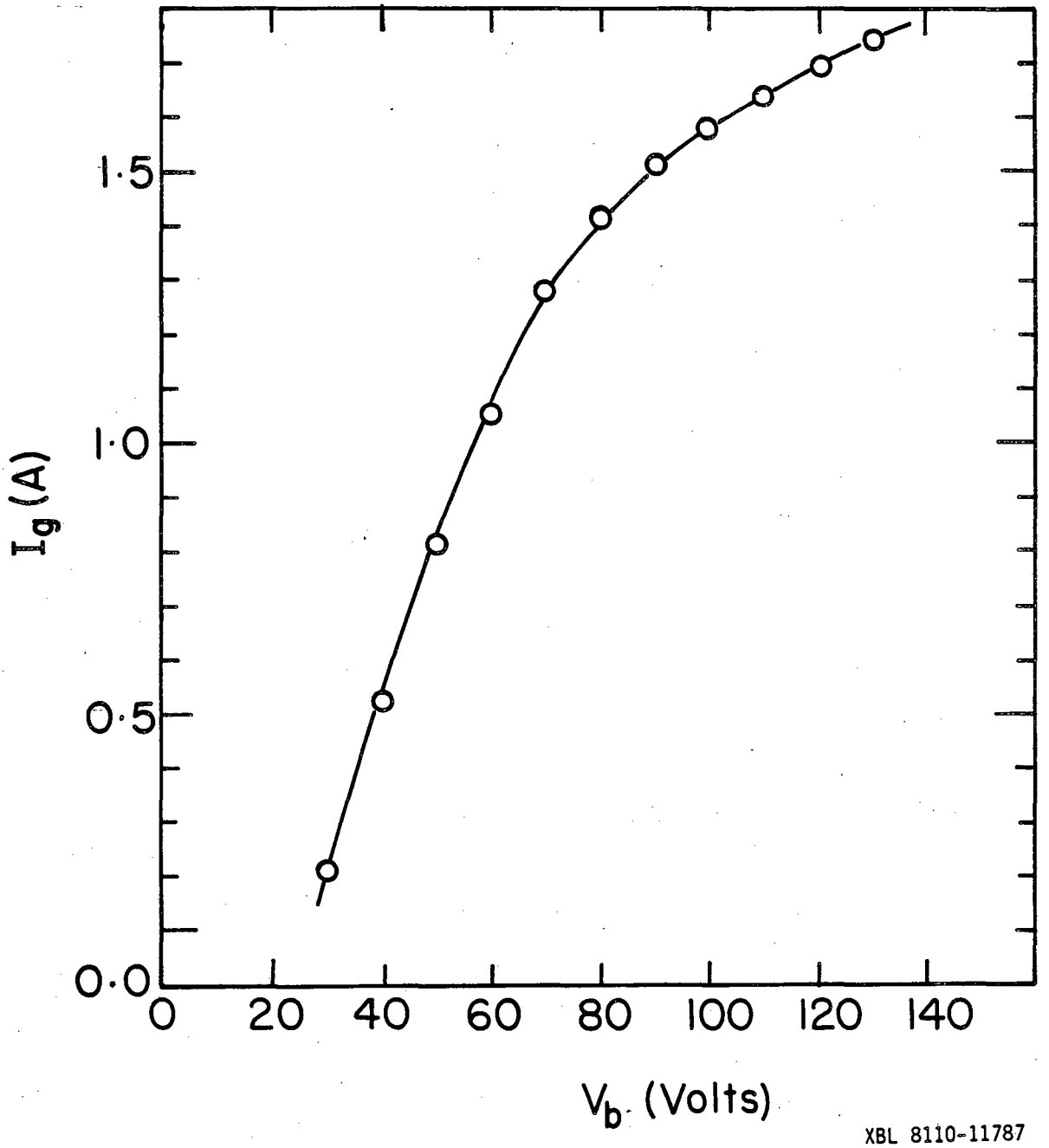


Fig. 5

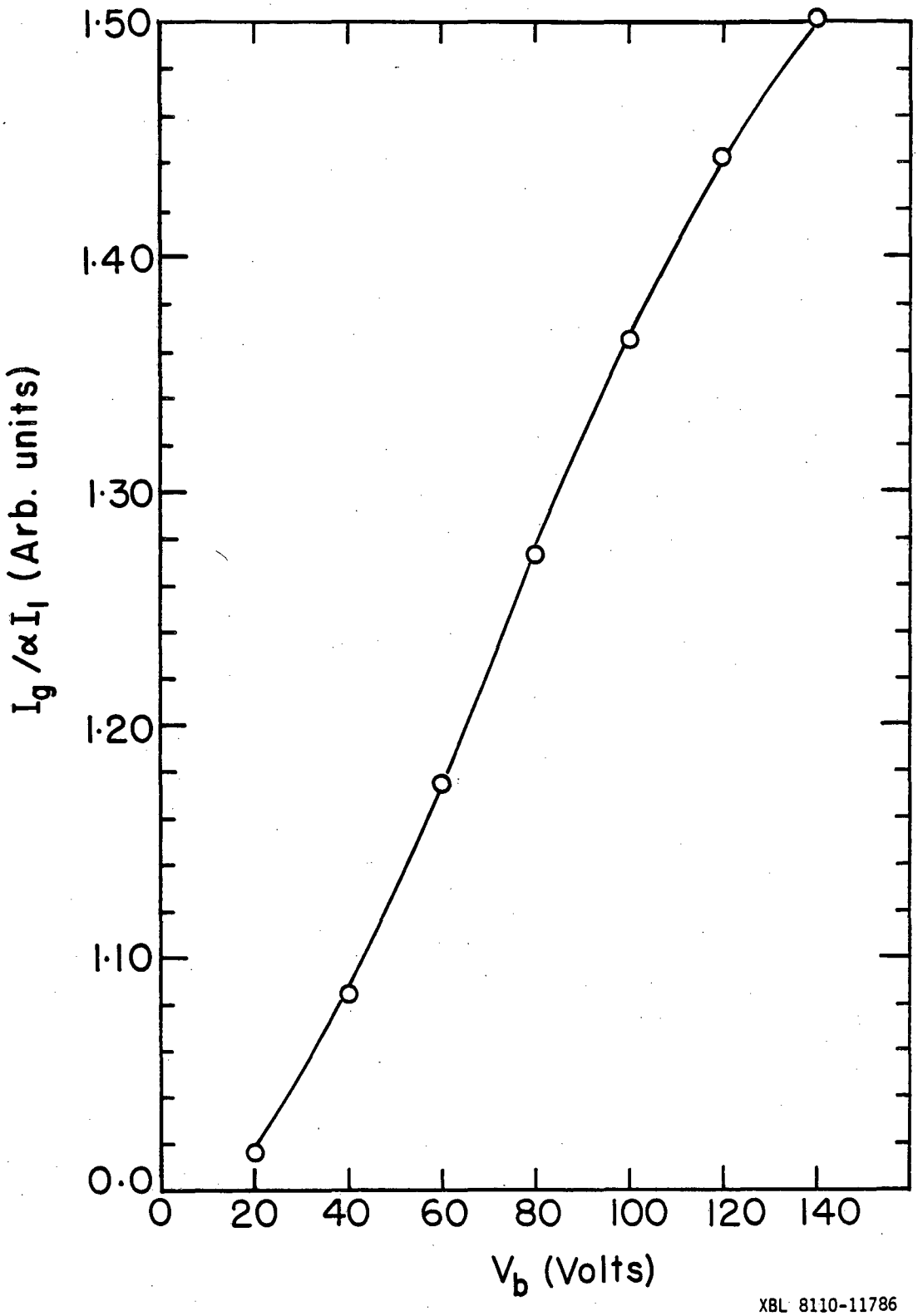
1·50
1·40
1·30
1·20
1·10
0·0
$I_g/\alpha I_1$ (Arb. units)
0
20
40
60
80
100
120
140
$V_b$ (Volts)
XBL 8110-11786

Fig. 6

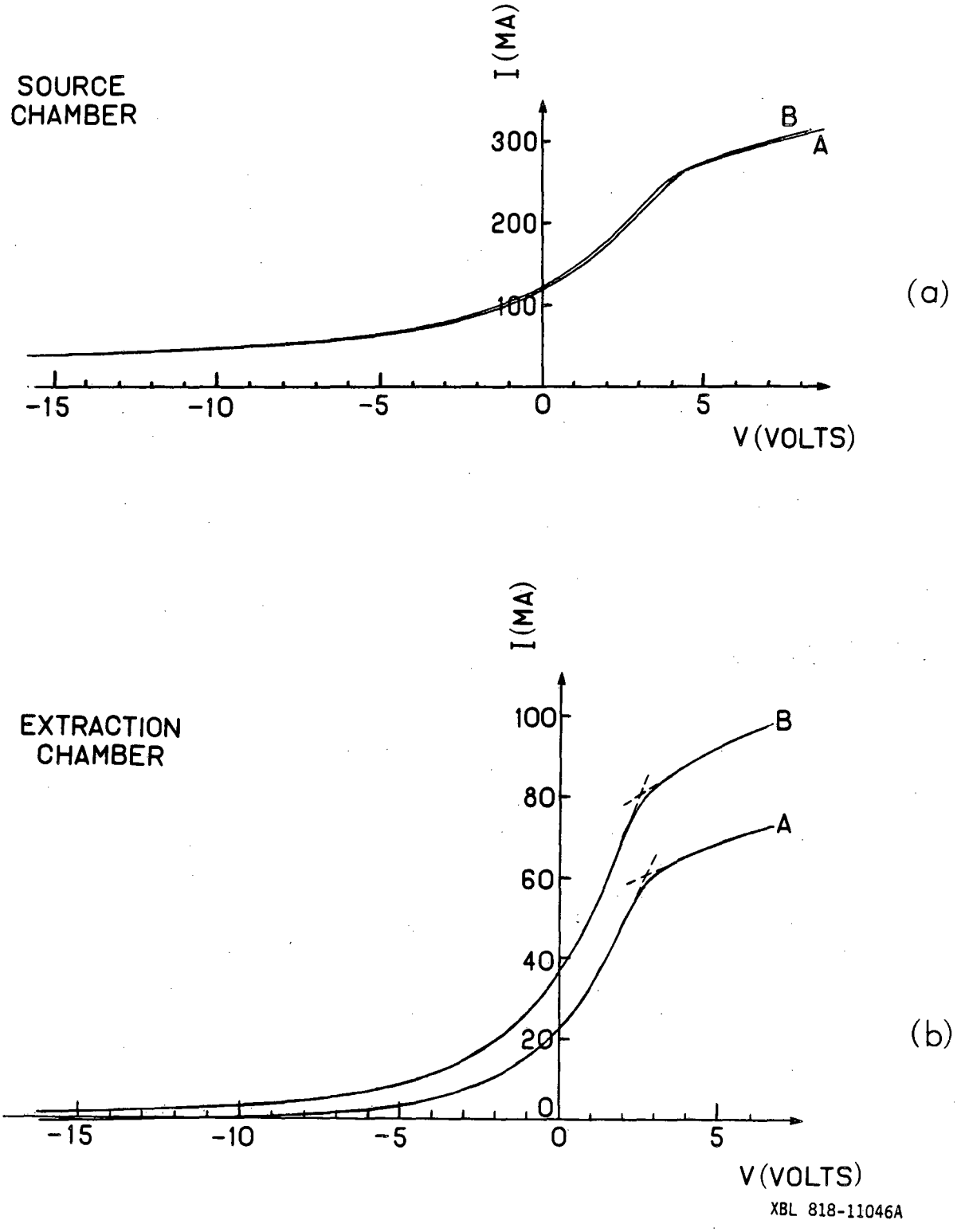
SOURCE
CHAMBER
I (MA)
300
200
100
B
A
-15
-10
-5
0
5
V (VOLTS)
(a)
EXTRACTION
CHAMBER
I (MA)
100
80
60
40
20
0
B
A
-15
-10
-5
0
5
V (VOLTS)
(b)
XBL 818-11046A

Fig. 7

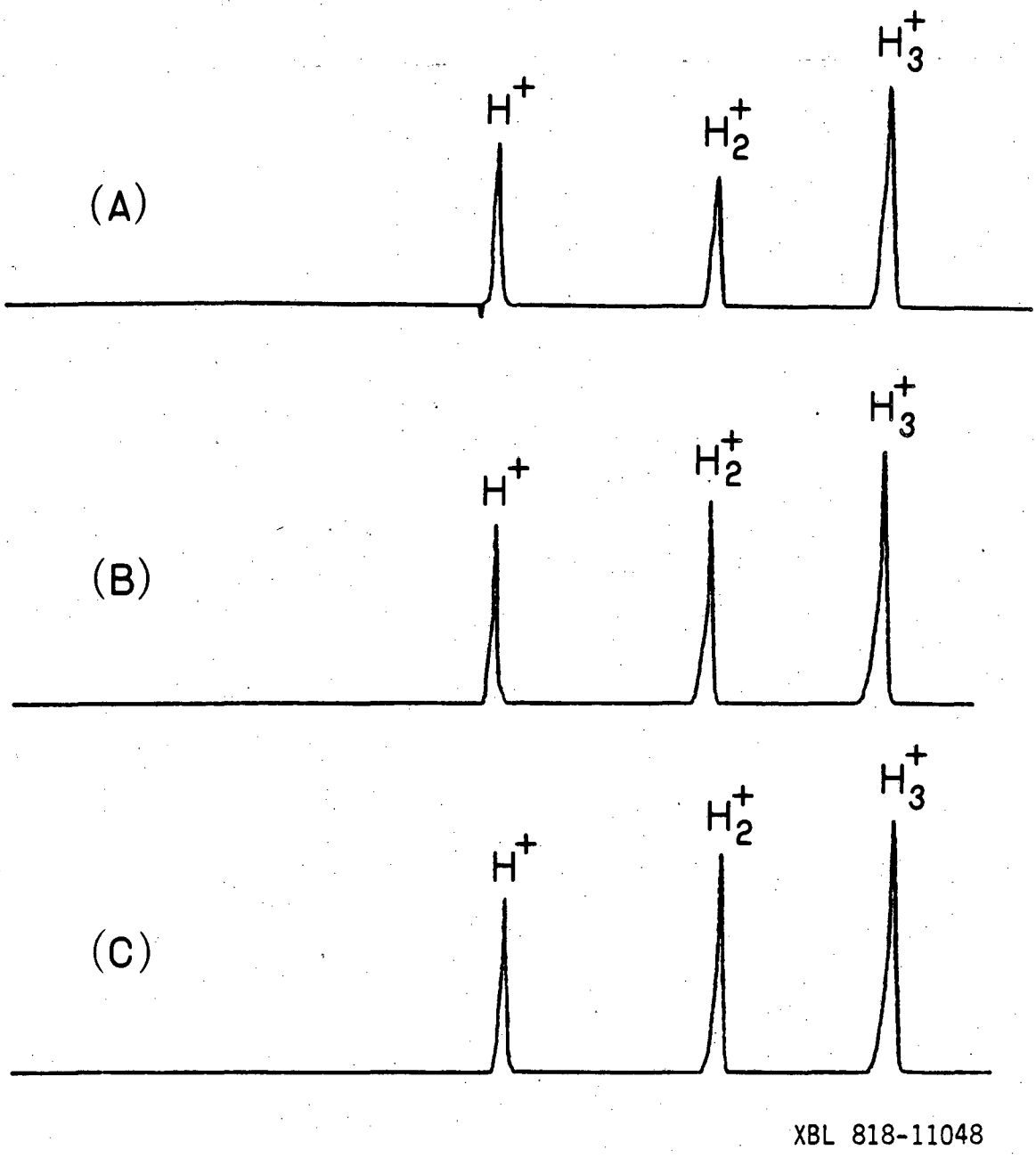


XBL 818-11048

Fig. 8

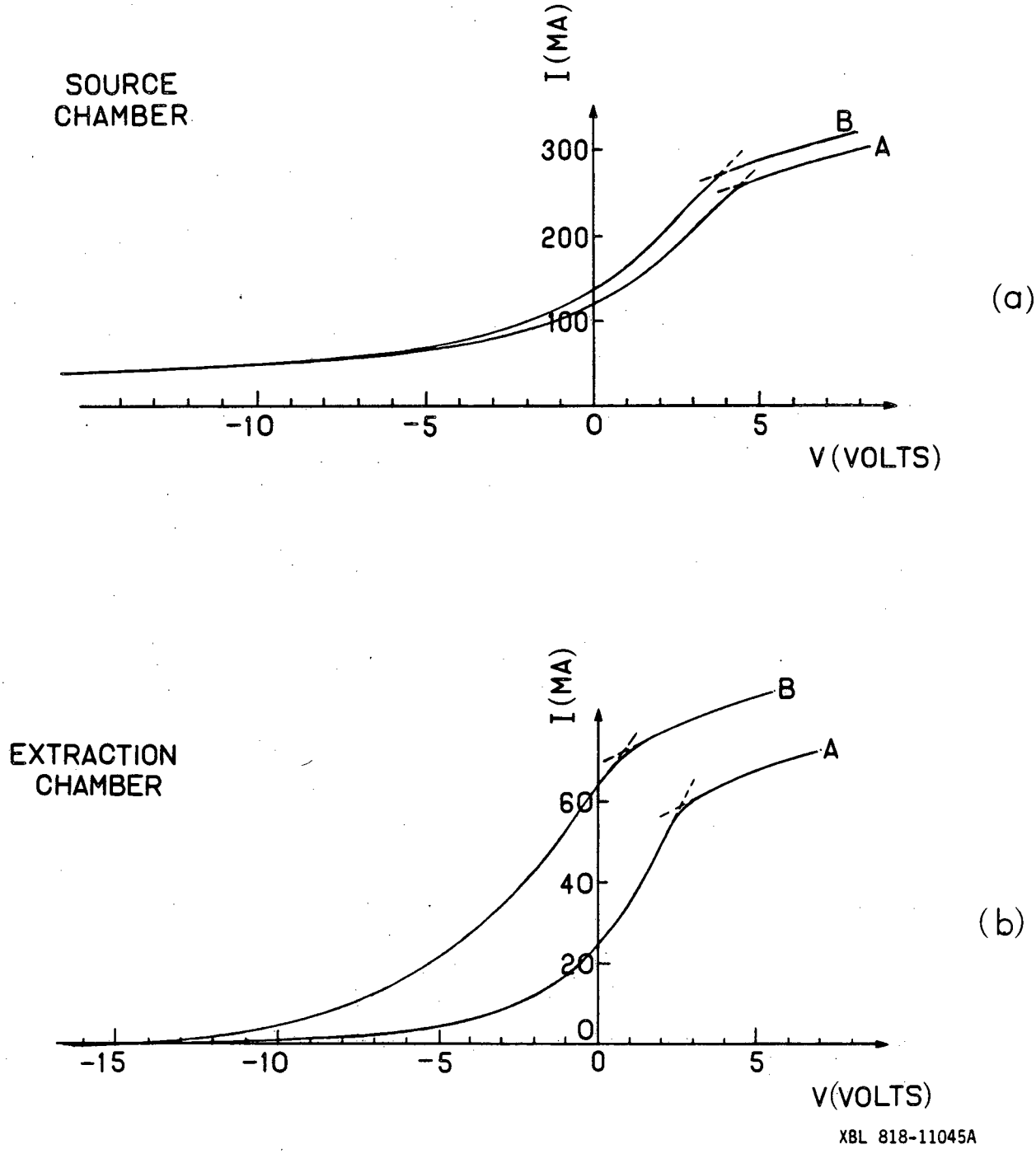
SOURCE
CHAMBER
I(MA)
300
200
100
B
A
-10
-5
0
5
V(VOLTS)
(a)
EXTRACTION
CHAMBER
I(MA)
60
40
20
0
B
A
-15
-10
-5
0
5
V(VOLTS)
(b)
XBL 818-11045A

Fig. 9

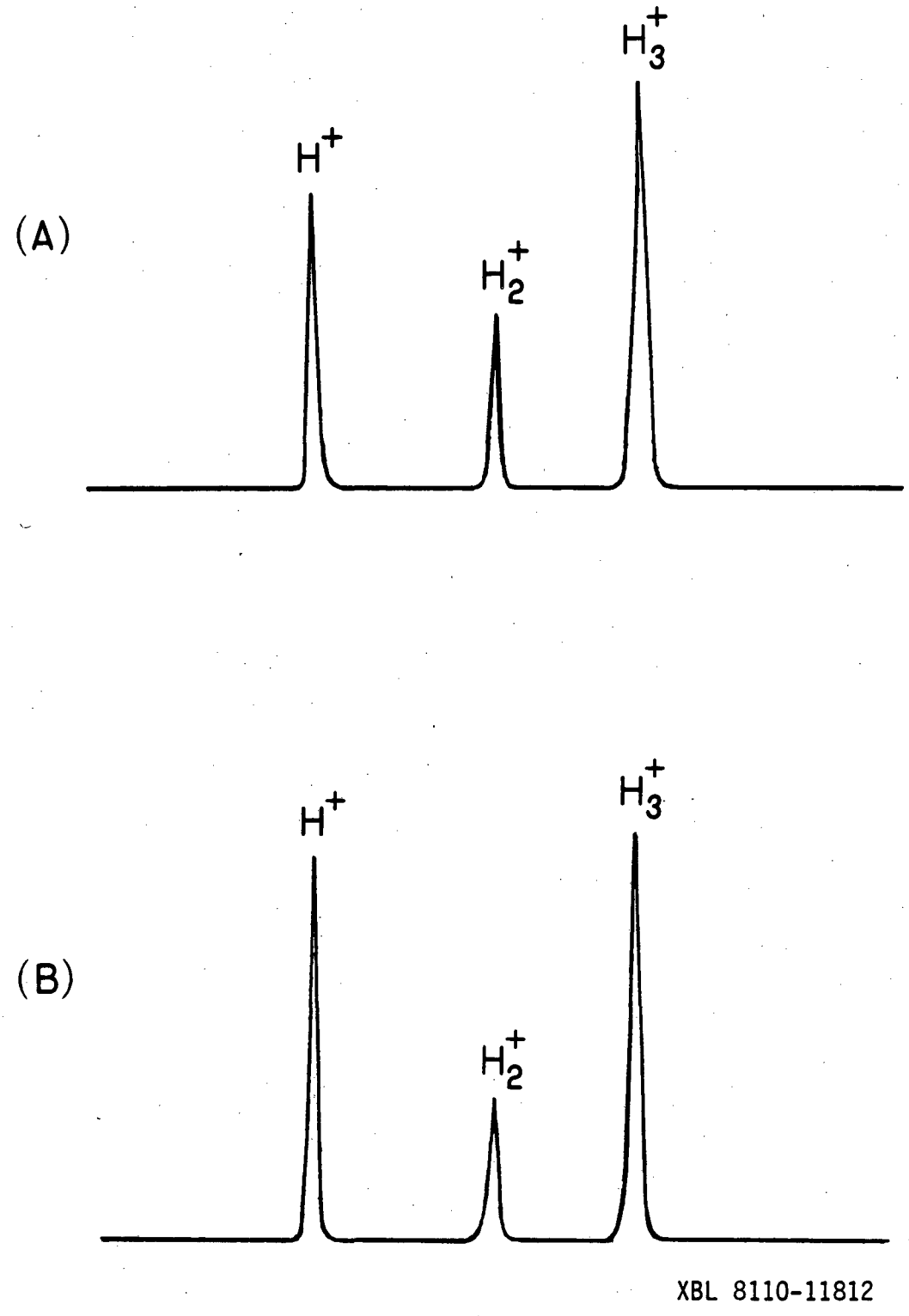


Fig. 10

*TECHNICAL INFORMATION DEPARTMENT*
*LAWRENCE BERKELEY LABORATORY*
*UNIVERSITY OF CALIFORNIA*
*BERKELEY, CALIFORNIA 94720*